A Synopsis of research work

for

Ph.D. Degree

by

Shibsankar Dutta

(Reg. No: R-14RS09110068)

Supervisor: Dr. Sukanta De

PRESIDENCY UNIVERSITY
KOLKATA

Institution: Presidency University

Department of Physics, 86/1 College Street,

Kolkata-700073, India

October 2018

A Synopsis of research work

for

Ph.D. Degree

Title: 2-D Nano Materials and their Hybrids as Supercapacitor Electrodes for Energy Storage Applications

Submitted by: Shibsankar Dutta

Supervisor: Dr. Sukanta De

Institution: Presidency University

Department of Physics, 86/1 College Street,

Kolkata-700073, India

Reg. No: R-14RS09110068

Email: shibsankar.rs@presiuniv.ac.in /shibsankar.05@gmail.com

Degree for which submitted: Doctor of Philosophy

Date of Registration: 12/08/2016

---------- ----------

Dr. Sukanta De

(Signature of Supervisor)

Shibsankar Dutta

(Signature of Candidate)

1. Introduction

Now a day, it is next to impossible to imagine our lives without wearable and portable electronic devices such as smart phones, laptops, e-papers, cameras, displays, transplantable medical devices, smart watch and many more, which play an effective role to change new generation's life style. With the decreasing availability of fossil fue1, increasing pollution associated with their use and ever growing demand of energy consumption of these kinds of smart electronics requires superior energy storage devices. According to Ragone chessboard, though supercapacitors (SCs) and batteries are the most successful players but due to the higher power density, cycle efficiency and charging-discharging rate supercapacitors plays leading role over other energy storage devices like lithium ion battery (LIB). [1]

On the basis of charge storage mechanism and used active electrode material supercapacitors can be classified into three types.[2] Most common type of SCs are electrochemical double layer capacitor (EDLC), which can store energy using ion adsorption and use carbon based active material like Graphene ,carbon nanotubes.[3-7] In transition metal oxides (TMOs), [8-16] transition metal dichalcogenides (TMDCs),[17] hydroxides [18-20] and conductive polymer[21-24] based supercapacitor energy is stored due to fast and reversible surface redox reaction occurring at the surface of the active electrode materials, which are known as pseudocapacitor (PSCs). Advanced approaches to increase the specific capacitance and energy density are to develop hybrid electrode materials for supercapacitor by adding electrochemically active materials with carbonaceous materials. This kind of SCs knows as Hybrid supercapacitors (HSCs).

Yet, a number of nano structured pseudocapacitive electrode materials such as nano particles, nanorods, nanospheres, nanosheets etc. have attracted for supercapacitor applications. Among them two dimensional (2-D) graphene analogues (GA) are the best for the highly flexible ultrathin-film supercapacitor in all-solid-state with higher energy density and excellent mechanical flexibility.[17,18,25]Two-dimensional (2D) nanomaterials offer exciting prospects for both fundamental studies and several technological applications due to their unique and intriguing properties.[26-30] Materials with intrinsic layered structure provide scope for the production of 2-D systems with a very broad range of properties. In their 2-D structure, inorganic layered materials such as transition metal oxides (MnO_2, RuO_2, MoO_3, TiO_2 etc) and transition metal dichalcogenides (MoS_2, WS_2, VS_2, etc) for their unique

properties becomes promising candidates for topological insulators, energy harvesters, thermal conductors, and transistors. [31-36]

The aim of this dissertation is to obtain a better understanding about the electrochemical behaviour of the 2D nano materials to fabricate of hybrid SCs with the carbonaceous electrode materials using aqueous and solid (gel electrolyte) electrolytes for two electrode and three electrode supercapacitor applications.

For the study, we have selected two dimensional transition metal oxides (TMOs), transition metal dichalcogenides (TMDCs), binary metal oxides and their composites or hybrids with Graphene and carbon nanotubes as electrode materials. Three different experimental techniques, namely, cyclic voltametry, galvanometric charging discharging and electrochemical impedance spectroscopy techniques were employed to investigate the nature of the supercapacitors.

Specifically, the work embodied in this thesis includes:

1. Hydrothermally Synthesized $BiVO_4$ –Reduced Graphene Oxide Nanocomposite as a High Performance Supercapacitor Electrode with Excellent Cycle Stability.

2. Scalable Mixed Solvent Assisted Transition Metal Oxides Nanosheets Exfoliations and Their Composites with SWCNT towards the Fabrication of Flexible Supercapacitors Endowed with High Energy Density.
3. MoS_2 Nanosheet/rGO Hybrid: An Electrode Material for High Performance Thin Film Supercapacitor.
4. Few layered vanadyl phosphate nano sheets-MWCNT hybrid as an electrode material for supercapacitor application.
5. Few-layered MnO_2/SWCNT Hybrid In-plane Supercapacitor with High Energy Density.

2. Review of status of Research

An electrode material plays an important role to improve the performance of supercapacitors. Last few decades it has been noticed that carbon based materials (carbon black, carbon nano tubes, graphene) is mainly used for EDLC supercapacitors, whereas conducting polymers, TMOs, TMDCs, phosphates were used for pseudo supercapacitors. Nanostructures of those materials including nano particles, nano wires, nano flowers, nano core-shell, and nano fibres and their composites with carbon based materials were already investigated as supercapacitor electrodes.[12,37-39] Chou et al. reported MnO_2 nanowires supercapacitors exhibits specific capacitance 167.5 F/g at 77mA/g current density.[37] M.Jin and his co-worker's reported PPy/MnO_2 particles based supercapacitor shows specific capacitance 110 F/g.[38] X. Lu et al. presented WO_{3-x}@Au@MnO_2 core shell supercapacitors exhibit specific capacitance 588F/g at10 mV/sec.[12] M.C.K. Sellers and his group already reported RuO_2/MWCNT supercapacitors with specific capacitance 96 F/g at 1 A/g current density.[39] As I mentioned earlier, among different nanostructures two dimensional nano materials become attractive electrode materials to achieve the flexible supercapacitors. And this is due to their unique properties such as

a. Two dimensional nanomaterials provide high specific surface area.

b. It provides macro mechanical flexibility to form thin films.

c. Atomically thick layer 2D materials have high electrochemical active sites.

d. Moreover, 2D materials possess confined thickness, which provide well-behaved electrical properties also.

Graphene was discovered experimentally in 2004,[40] and after that graphene becomes the first choice for the EDLC supercapacitor electrode materials to the researcher but restacking properties of graphene sheets plays a negative role due to which graphene based supercapacitors does not provides expected results. The theoretical value of the graphene based supercapacitor is 550F/g whereas reported values are in the range from 80 to 118 F/g.[41] Even the reported specific capacitance value (220 F/g at 1 A/g) for the 3D graphene hydrogels based three electrode supercapacitor is much lower than the theoretical value.[42] In last few years lots of work has been already done to improve the performance of supercapacitor by introducing 2D TMOs, TMDCs to the carbon based materials. L. Peng et al. reported MnO_2 nanosheets / graphene based supercapacitor delivered specific capacitance 267 F/g at 0.2 A/ g.[16] Ultrathin

MoO_3 nano crystals self-assembled on graphene nanosheets based solid state supercapacitor obtained specific capacitance 373 F/g at 1 A/g.[43] Co-Al hydroxide nanosheets/graphene supercapacitor obtained specific capacitance 880 F/g at 5 mV/s.[44] $VOPO_4$ nanosheets/graphene based thin film two electrode supercapacitor delivered 8360.5 mF/cm2 specific capacitance.[45] J. Feng and his co-worker reported VS_2 nano sheets based supercapacitor shows capacitance value 4760 μF/cm^2.[17] Though lots of composite and hybrid electrode materials already studied but most of cases energy density was below the expected level.

Present work reported large scale production of 2D materials using mixed solvent exfoliation from their bulk forms and Hydro (or solvo) thermally synthesized layered materials also exfoliated by liquid phase exfoliation by suitable solvents. These well dispersed stable solutions were used to make thin films which can be readily transferred on wide range of substrates for flexible supercapacitor electrode applications with high energy density. The performance of the composite electrode materials by varying compositions also included in the present work.

3. Experimental techniques for studying electrochemical performances of supercapacitors

In the present study we have done cyclic voltammetry, galvanometric charging discharging and electrochemical impedance spectroscopy to investigate the performance of supercapacitors using CHI 600E Series Electrochemical Analyzer/Workstation.

A brief description of the methods employed is given below:

(a) Cyclic voltammetry:

Cyclic voltammetry is a well-known technique to study the electrochemical performance of supercapacitors, in which a potential is applied to the working electrodes at a constant rate and current flowing through the electrode is measured over a specified potential window. EDLCs shows rectangular shaped CV curves whereas PSCs shows redox peaks in their CV curves.

The specific capacitance of the two electrode symmetric and asymmetric supercapacitors can be calculated from the CV curves using equations (1) and (2) respectively, where m is the total mass of the electrode materials, ν (V/s) is the scan rate and ΔV represent potential window. Energy density (E) and power density (P) can also be calculated from the equations (3) and (4) for symmetric supercapacitor and that for asymmetric supercapacitor from equations (5) and (6). [45-47]

$$C_{symmetric} = \frac{4 \int I_1 \, dV}{\nu m \Delta V} \ldots\ldots\ldots\ldots\ldots (1)$$

$$C_{asymmetric} = \frac{2 \int I_1 \, dV}{\nu m \Delta V} \ldots\ldots\ldots\ldots\ldots (2)$$

$$E_{symmetric} = \frac{1}{8} C(\Delta V)^2 \ldots\ldots\ldots \quad (3)$$

$$P_{symmetric} = \frac{1}{8} C \, \Delta V \nu \quad \ldots\ldots\ldots\ldots (4)$$

$$E_{asymmetric} = \frac{1}{4} C(\Delta V)^2 \ldots\ldots\ldots \quad (5)$$

$$P_{asymmetric} = \frac{1}{4} C \, \Delta V \nu \quad \ldots\ldots\ldots\ldots (6)$$

(b) Galvanometric charging discharging (GCD):

In GCD measurements a constant current density is applied between the electrodes until the lower or higher potential is reached. We can also calculate the specific capacitances from the GCD curves according to the equations (7) and (8) for symmetric and asymmetric two electrode supercapacitors respectively, where m is the total mass of the electrode materials, I is the applied current and $\Delta V/\Delta t$ represent slope of the discharge curves after IR drop. [45] The internal resistance of the supercapacitors can also be calculated from the very short IR drop, which is obtained in the initial portion of the discharge curves. For EDLC rest of the discharge curve after IR drop is linear and that for PSCs and HSCs large deviations in linearity occurs.

$$C_{symmetric} = \frac{4I\,\Delta t}{m\,\Delta V} \ldots\ldots\ldots\ldots\ldots (7)$$

$$C_{asymmetric} = \frac{2I\,\Delta t}{m\Delta V} \ldots\ldots\ldots\ldots\ldots (8)$$

(c) Electrochemical impedance spectroscopy (EIS):

Kinetic parameters of the electrochemical processes such as charge transfer, ion diffusion can easily determine by the electrochemical impedance spectroscopy technique, where the impedance data are recorded at the open circuit voltage by applying a small alternating voltage ($\pm$ 5mV to ± 10 mV) over a frequency window (1mHz to 1MHz).The series resistance (R_s) and charge transfer resistance (R_{ct}) can be calculated from the EIS graph (Nyquist plot).The diameter of the semicircle in the medium frequency region represent the value of R_{ct}, Low value of R_{ct} indicates fast electrochemical reactions. An inclined line a in the low frequency region displays Warburg impedance. From the linear part of the Bode plot (log |Z| vs. log n curve) capacitance value can also be calculated from the equation (9), where |Z| and n represent the imaginary part of impedance and frequency respectively. [48] The Bode plots show that capacitance value decreases with the increasing frequency because at high frequency electrolyte ions cannot penetrate into the microspores.

$$C = \frac{1}{2\pi f|Z|} \ldots\ldots\ldots\ldots\ldots (9)$$

4. Work Done

1) Hydrothermally Synthesized $BiVO_4$–Reduced Graphene Oxide Nanocomposite as a High Performance Supercapacitor Electrode with Excellent Cycle Stability.

We have synthesized bismuth vanadate ($BiVO_4$) by a simple hydrothermal method.We have prepared a set of samples by varying reaction time.Henceforth, we designate the samples corresponding to 30 min, 60 min, 90 min and 120 min reaction span as B-30, B-60, B-90 and B-120 respectively. We have studied the cyclic voltammetry (CV) performances of the B-30, B-60, B-90 and B-120 samples at 5 mV/s scan rate in two electrode configuration using both 1M Na_2SO_4 aqueous electrolyte and PVA/H_2SO_4 gel as solid electrolyte. Amongst the all samples, B-90 exhibits superior electrochemical performance due to their high surface area and well crystalline nature which is obvious from our FESEM and XRD results shown in the figure1 and figure2 respectively.

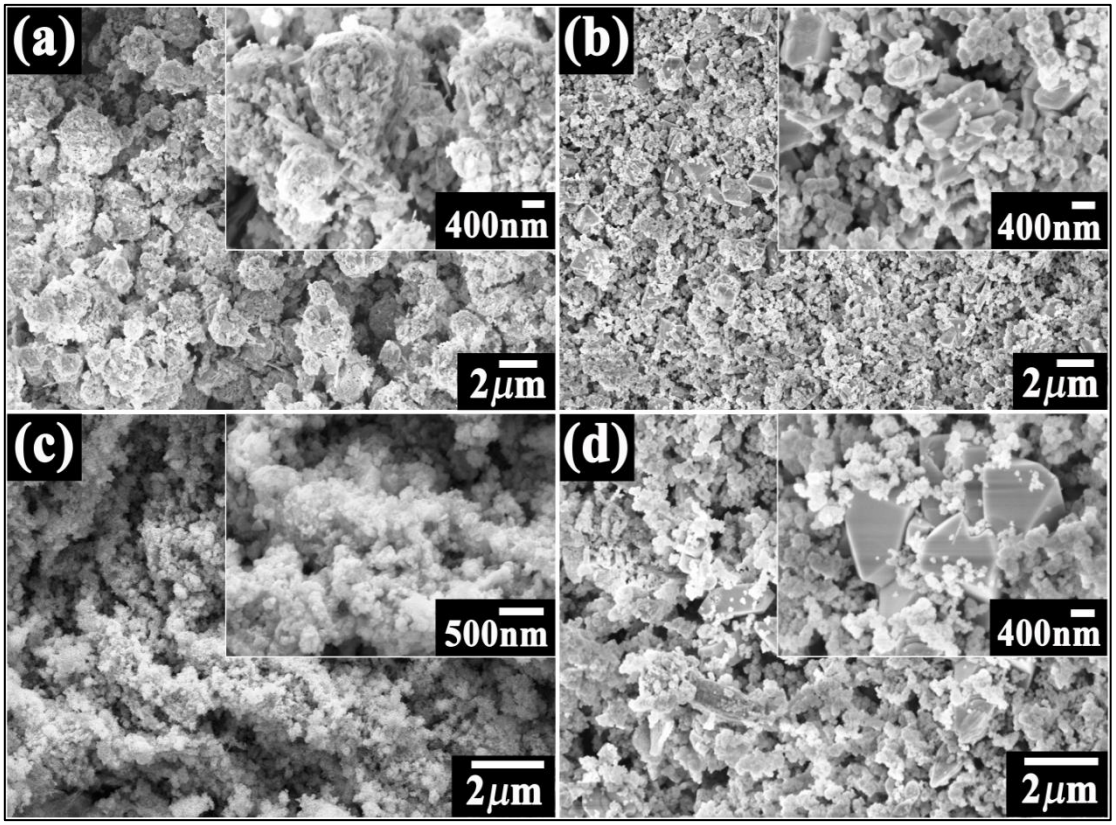

Figure 1: FESEM images of (a) B-30, (b) B-60, (c) B-90 and (d) B-120 samples; insets showing their high magnification view.

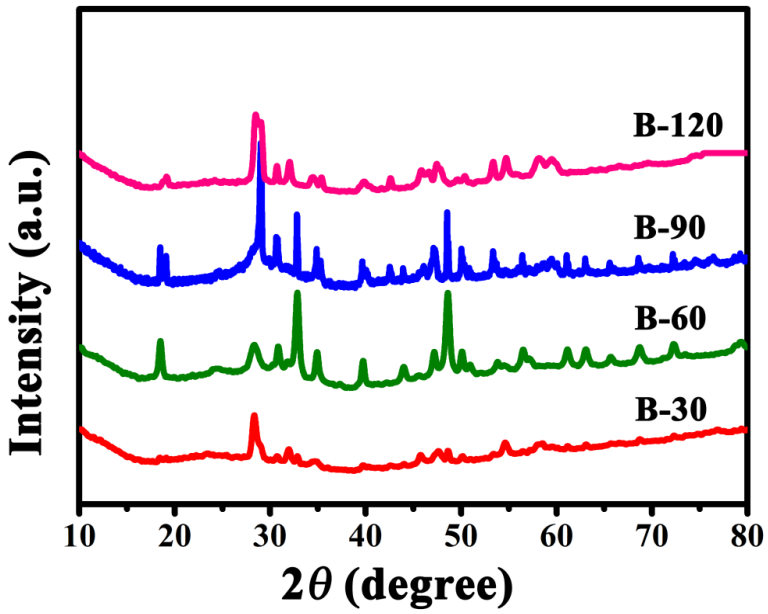

Figure 2: XRD pattern of $BiVO_4$ samples synthesized at different reaction time

For further electrochemical study we choose B-90 sample due to their superior electrochemical performance over the other prepared sample. We have also prepared different $BiVO_4$/rGO hybrids; different concentration of GO solution (20 mL, 40 mL and 60 mL) with initial concentration (1mg/mL) was added to the above mentioned mixture. Henceforth we denote the $BiVO_4$/rGO samples using 20 mg, 40 mg and 60 mg of GO contents as the BG1, BG2 and BG3 sample. FESEM image of the BG1, BG2 and BG3 samples are shown in the figure 3.

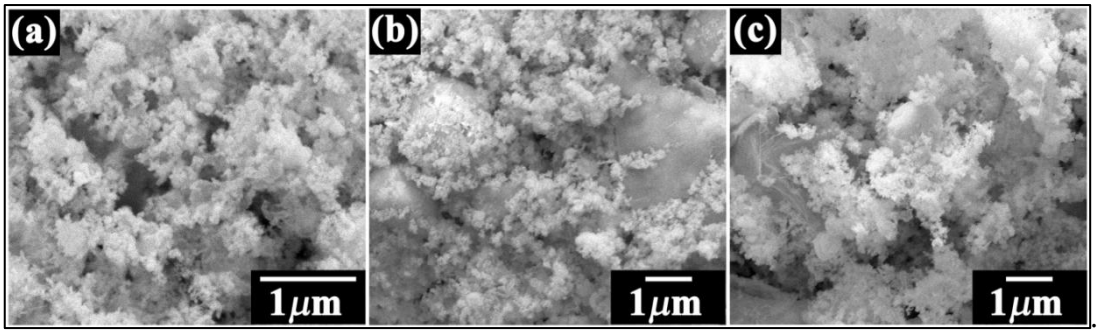

Figure 3: FESEM images of (a) BG1, (b) BG2, (c) BG3 samples.

Amongst the all samples, BG2 exhibits superior electrochemical performance both in presence of 1M Na_2SO_4 aqueous electrolyte and PVA/H_2SO_4 gel electrolyte. CV curves at different scan rates and charging discharging of B-90 and BG2 samples are shown in Fig.4. The obtained maximum specific capacitance value is 400 F/g at 5 mV/s scan rate for the

hybrid electrode materials in presence of PVA/H_2SO_4 gel electrolyte and that in presence of 1M Na_2SO_4 is 245 F/g at 5mV/s scan rate. The result clearly shows better performance of the electrodes in presence of PVA/H_2SO_4 gel electrolyte. The presence of –OH groups of PVA may absorbs large water contents and enhances the ionic conductivity of the electrolyte as well as the electrochemical performances. BG2 symmetric supercapacitor shows excellent stability, retains its 98% initial capacitance after 1000 cycles. The obtained energy density for hybrid electrode is 35.37 Wh/kg at power density 2.05kW/kg.

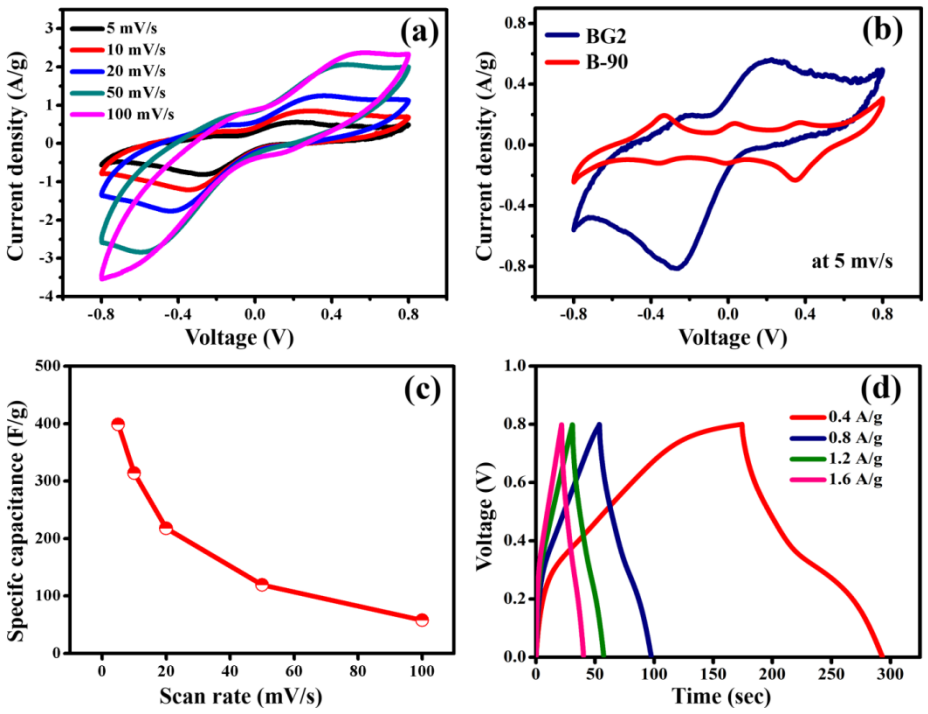

Figure 4. CV graph of (a) BG2 at different scan rates, (b) B-90 and BG2 at 5mV/s respectively, (c) scan rate vs specific capacitance graph of BG2, (d) galvanometric charging discharging graphs of BG2 at different current density.

2) Scalable Mixed Solvent Assisted Transition Metal Oxides Nanosheets Exfoliations and Their Composites with SWCNT towards the Fabrication of Flexible Supercapacitors Endowed with High Energy Density

Transition metal oxides (TMOs) are exfoliated by a simple mixed solvent assisted ultrasonic method using the proper composition of ethanol and water, both have low boiling point, volatile in nature. In this method we have produced a stable dispersion of TMOs nanosheets.To analyze quantitatively, we have recorded absorption spectra for all dispersions and took the measured of absorbance per unit cell length (A/l) at 375 nm, 380 nm and 450 nm

for MoO_3, MnO_2 and RuO_2 respectively which can be used as metric to determine the concentration of TMOs in dispersion. The variation of A/l with volume fraction of ethanol in water (Figure.5 (a-c)) clearly shows that pure ethanol or pure water hardly can disperse oxide materials but the concentrations of TMOs dispersions are directly dependent on the volume fraction of ethanol in water with peak at 65% ethanol in water for MoO_3. Whereas for both MnO_2 and RuO_2 peak value of A/l is at 50% mixed solvent. Such composition-dependent dispersion results can be explained by the theory of Hansen Solubility Parameters (HSP). [49, 50] The obtained concentration of dispersed MoO_3 to be 0.33 mg/ml with initial concentration 20 mg/ml, which is almost 3 times higher than that of in IPA ,[51]even the initial concentration was 15 times lower in our case and the concentration of MnO_2 and RuO_2 (C_i=20 mg/ml) was 0.22 mg/ml and 0.23 mg/ml respectively. These well dispersed stable solutions were used to make thin film of TMOs nanosheets which can be readily transferred on wide range of substrates for different applications. The atomic force microscopy (AFM) images shown in Fig. 5(d-f) of the metal oxides clearly revealed the presence of nanosheets of the metal oxides with an average thickness of 1.85 nm for MoO_3, 1.07 nm for MnO_2 and 2.1 nm for RuO_2 respectively, denoting that our exfoliated metal oxides are mostly bi-layers. [52-54] HRTEM study reveals that the nanosheets are mostly bi-layer with average lateral size of 300 nm for MoO_3 and 200 nm for MnO_2 and RuO_2 respectively. In all cases, a large numbers of quasi-2D nanosheets were seen, with typical example as shown in Fig. 6(a-c). Further the SAED patterns of all TMOs (insets of Fig. 6d-f)) indicate their single crystalline nature.

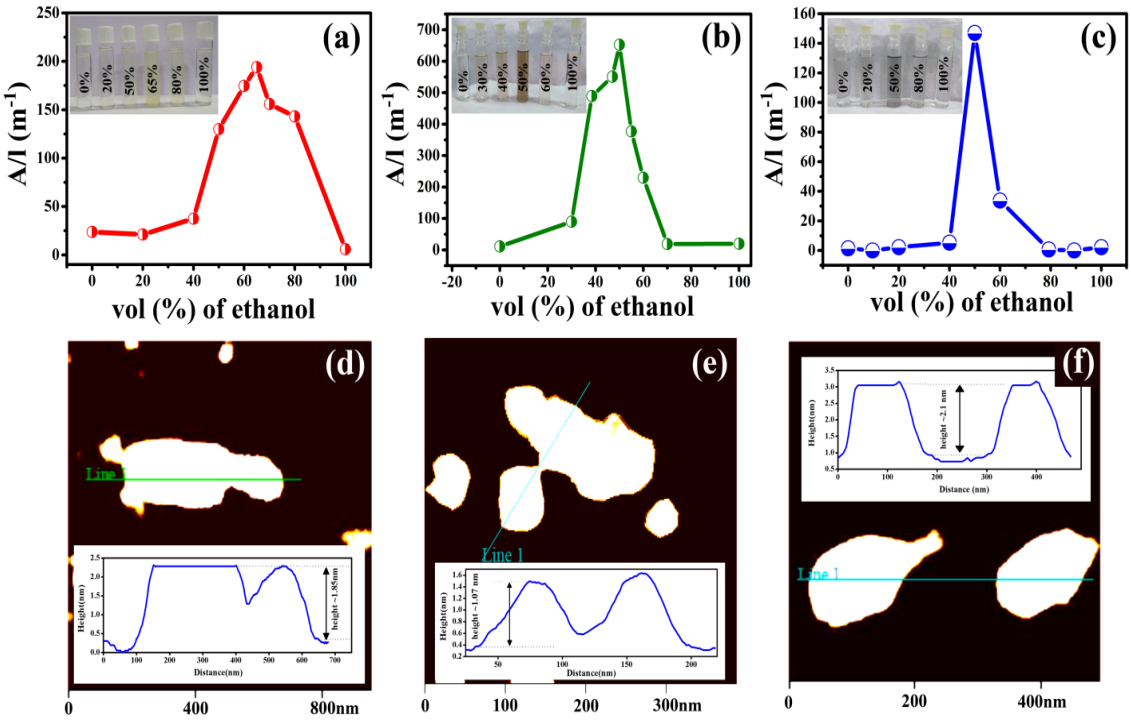

Figure 5. (a-c) Graph of A/l vs volume fraction (ethanol) in water for the MoO_3, $MnO_2$and RuO_2 nanosheets respectively; Inset showing their corresponding digital images of different vol% EtOH; (d-f) Atomic force microscopy (AFM) analysis of MoO_3, MnO_2 and RuO_2 respectively.

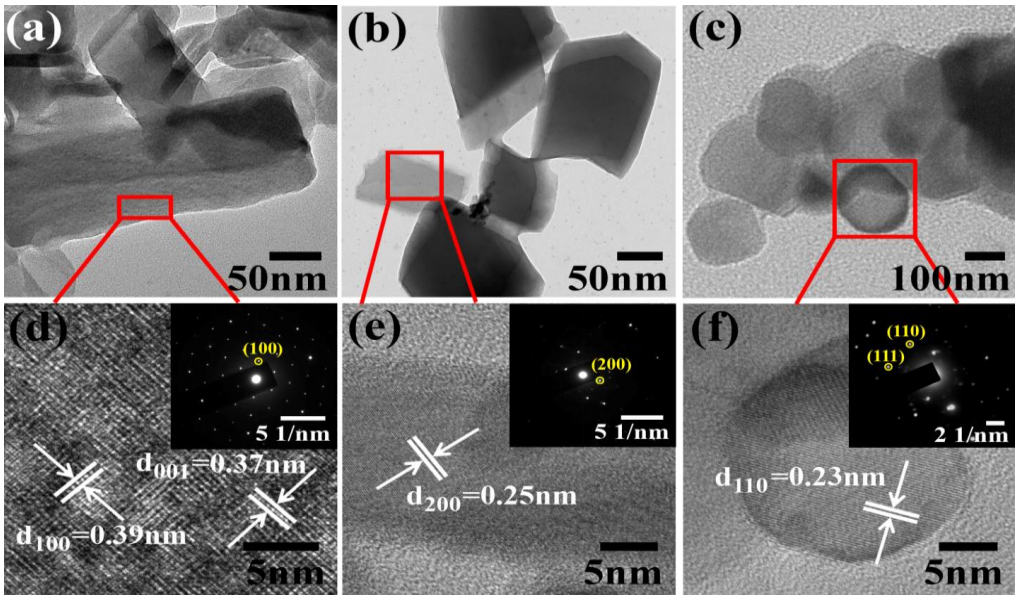

Figure 6. (a-c) Transmission electron microscopy (TEM) images and (d-f) high-resolution TEM analysis with selected area electron diffraction (SAED) pattern in the inset of MoO_3, MnO_2 and RuO_2 respectively.

These well dispersed stable solutions were used to make thin film of TMOs nanosheets which can be readily transferred on wide range of substrates for different applications. Composite thin film of TMOs nanosheets with SWCNT (25 wt%) deposited of gold coated PET for device fabrication. The symmetric solid state supercapacitors were prepared by these thin films with polyvinyl alcohol PVA-H_2SO_4 gel as a solid electrolyte. Cyclic voltammetry (CV) graph of the two electrode measurement for the composite electrode materials over the voltage window -0.8V to +0.8 V shown in the Fig. 7(a-c) at 5, 10, 20, 50, 100 mV/s scan rates. Galvanometric charging discharging performances of the two electrode system were also studied and are shown in the Fig. 7(d-f). As fabricated thin film symmetric supercacitors exhibit high specific capacitance (709.61F/g, 529F/g and 638 F/g for MoO_3-SWCNT, MnO_2-SWCNT and RuO_2-SWCNT respectively), excellent flexibility and long cycle life, leading to an extremely high energy density (63.11Wh/Kg at 2.554 kW/kg, 47.02 Wh/Kg at 1.904 kW/Kg and 56.71Wh/Kg at 2.296 kW/Kg). Our findings represent a promising direction and

significant steps towards exfoliating TMOs to produce 2D oxide nanosheets in low toxic mixed solvent for flexible energy storage device with high energy density.

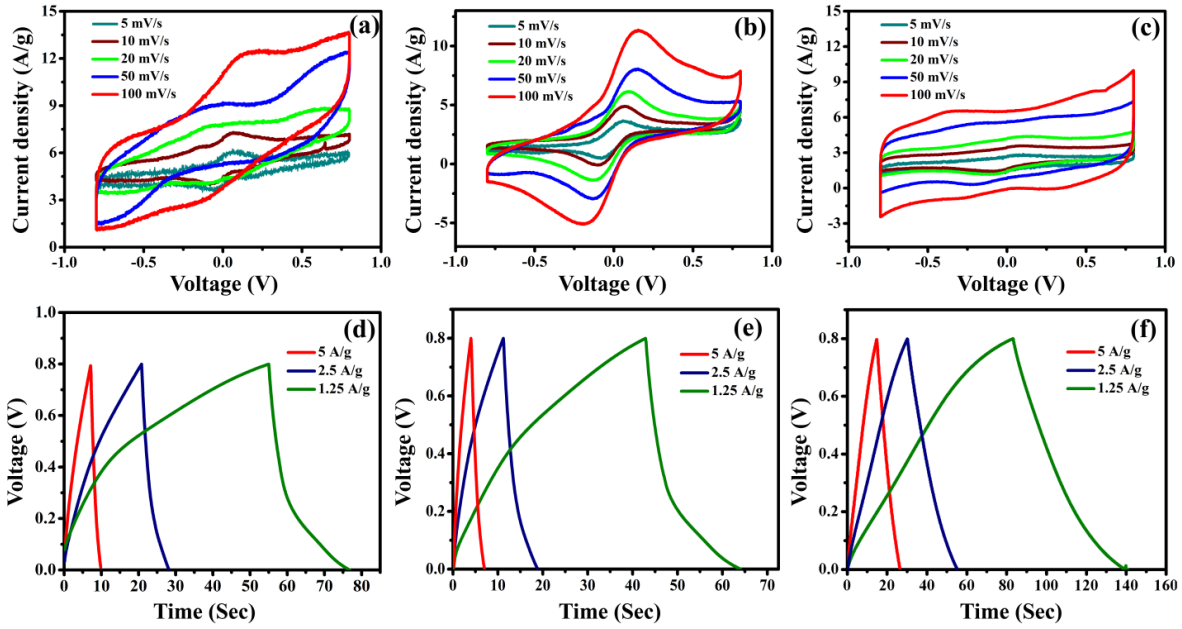

Figure7. Cyclic voltammetry graph of (a) MoO_3/SWCNT, (b) MnO_2/SWCNT and (c) RuO_2/SWCNT at different scan rates respectively; Galvanometric charging discharging graphs of (d) MoO_3/SWCNT, (e) MnO_2/SWCNT and (f) RuO_2/SWCNT at different current density respectively.

We have investigated the behaviour of our symmetric supercapacitors under a variety of bending conditions. The cyclic voltammetry of the solid state supercapacitors at different bending angle are shown in the Figure 8(a-c). The electrochemical performances of the device do not significantly change under various bending conditions. The specific capacitance values of the all the devices are almost remain same during bending, which is displayed in the Figure 8d.

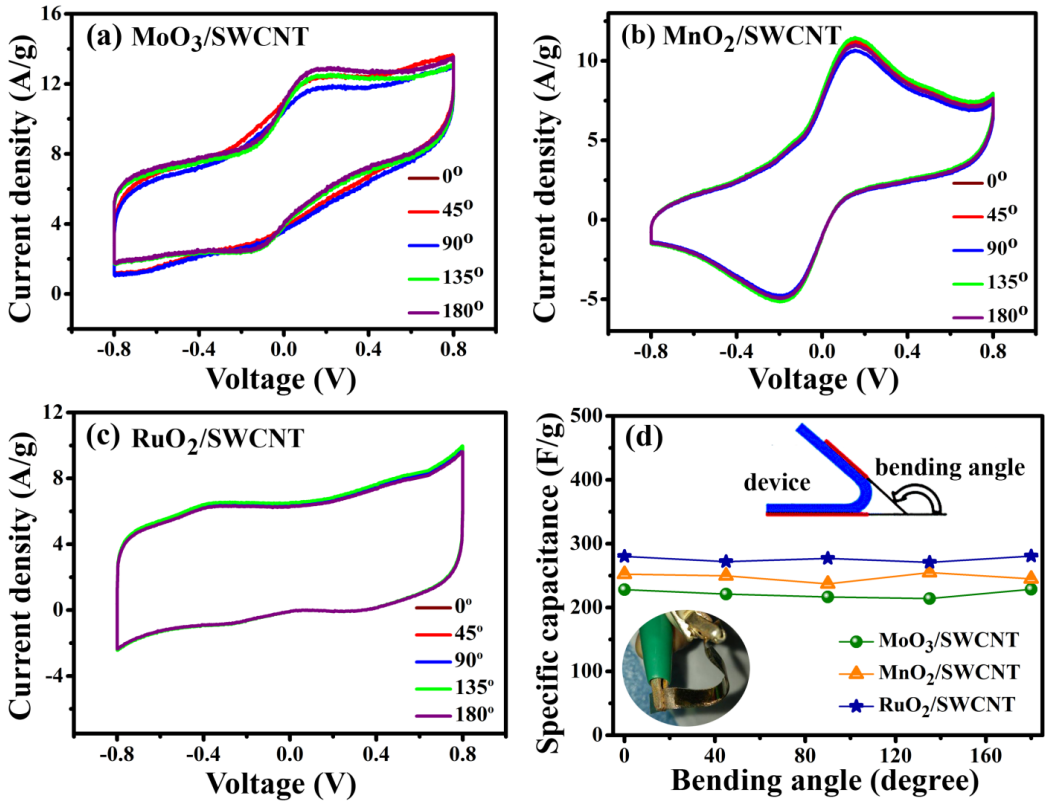

Figure8. Cyclic voltammetry curves at different bending conditions at 100 mv/s scan rate for (a) MoO_3/SWCNT, (b) MnO_2/SWCNT and (c) RuO_2/SWCNT respectively. (d) Specific capacitance vs bending angle graph of all TMOs/SWCNT composite.

3) MoS_2 Nanosheet/rGO Hybrid: An Electrode Material for High Performance Thin Film Supercapacitor.

Two-dimensional nano materials like Graphene and transition metal dichalcogenides are the suitable choice for the supercapacitor application due to their interesting properties including high surface area. MoS_2 nanosheets and MoS_2/rGO hybrid were synthesized by simple hydrothermal route. The FESEM images of MoS_2 and MoS_2/rGO hybrid shown in the figure 9(a), (b) respectively, which conforms the formation of two dimensional nano sheets of the as prepared samples. The inset figure of figure 9(b) shows the presence of rGO clearly in the hybrid sample. Transmission electron microscope (TEM) image of the MoS_2 is taken on a holy carbon coated grid as shown in the figure 9(c) which shows sheet like structure of MoS_2 with lateral dimension of <500 nm long and the Atomic force microscope image of the MoS_2 shown in the figure 9(d), indicates the thickness of MoS_2 nanosheet is 1.09 nm.

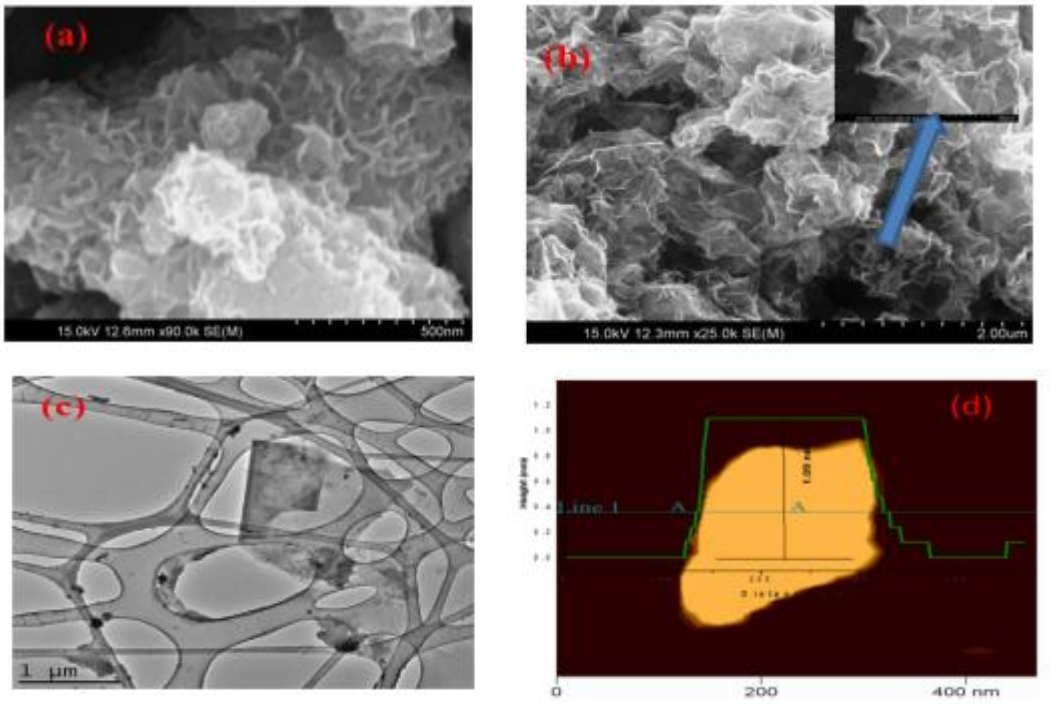

Figure 9. (a)FESEM images of MoS_2, (b) MoS_2 /rGO, (c) TEM image of MoS_2, and (d) AFM image of MoS_2 nano sheet.

To prepare thin film of MoS_2 and MoS_2/rGO hybrid, we have exfoliated as-prepared hydrothermal products in NMP followed by vacuum filtration on the cellulose membrane. After that the films were transferred on the Au coated PET for further use as a working electrode.

All electrochemical studies were carried out in a three electrode cell system using MoS_2 and hybrid film as a working electrode, platinum wire as a counter electrode, and a Ag/AgCl as a reference electrode with 1M H_2SO_4 aqueous solution as the electrolyte. All the electrochemical analysis including cyclic voltammetry (CV), galvanometric charging–discharging (CD), was carried out on CHI 660E electrochemical workstation.

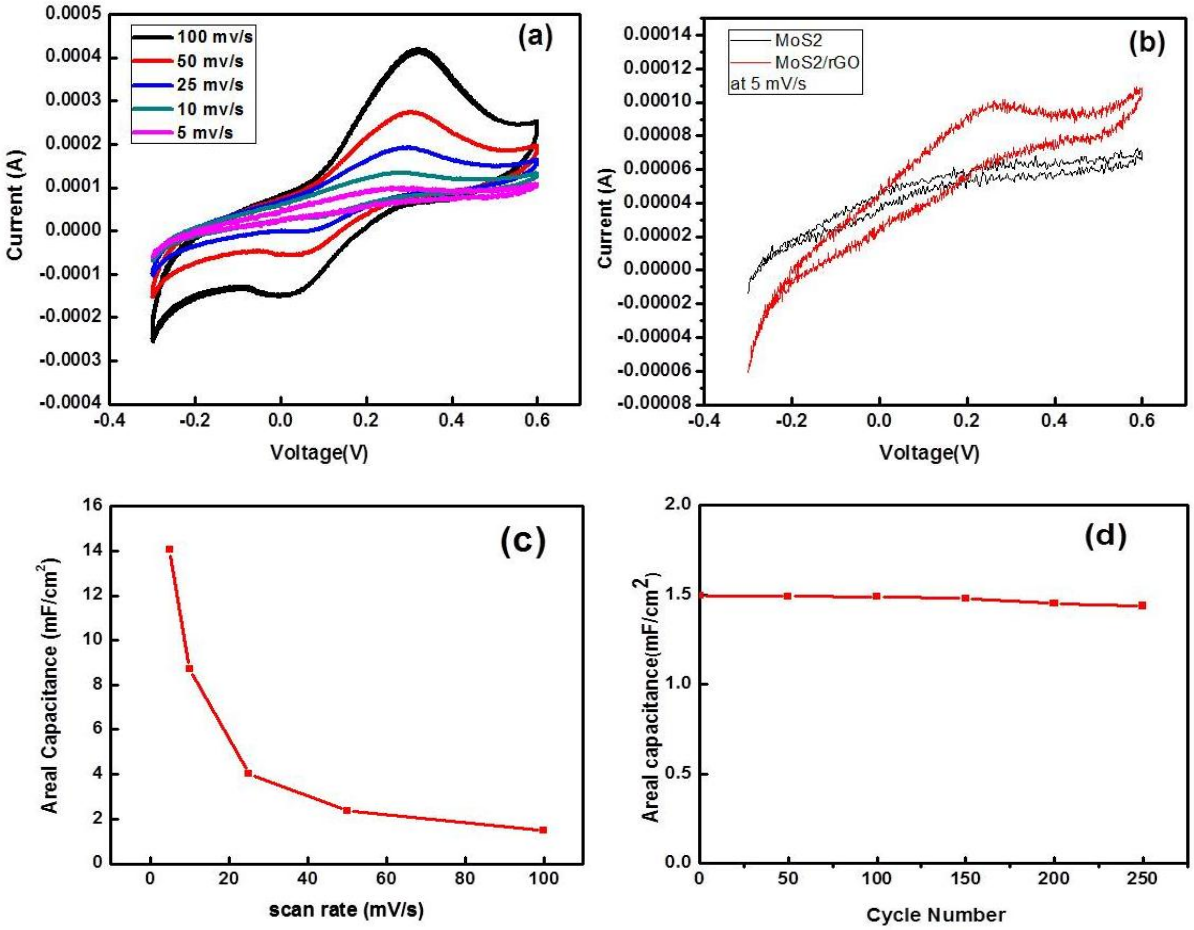

Figure10. (a) CV graph of Hybrid materials at different scan rates,(b) CV graph of Hybrid materials and MoS_2 at 5 mV/s scan rate,(c)Areal capacitance vs scan rate graph of Hybrid material,(d) C/C_0 vs cycle number graph of hybrid material at 100mV/s.

The electrochemical performance of the electrode materials have been investigated measuring the cyclic voltammetry using three electrode system at different scan rates from 5 mV/s to100 mV/s with 1M H_2SO_4 aqueous solution as the electrolyte as shown in the figure 10(a). The areal capacitances of the hybrid electrode materials calculated from the CV curves to be 14.09mF/cm^2, 8.73 mF/cm^2, 4.025 mF/cm^2, 2.373mF/cm^2, and 1.501mF/cm^2 at 5, 10, 25, 50 and 100 mV/sec scan rates respectively. However the value of areal capacitance for MoS_2 electrode at 5 mV/s scan rate is 0.79mF/cm^2. The corresponding obtained specific capacitance values are 607 F/g, 376 F/g, 173 F/g, 102 F/g, and 64 F/g at scan rates 5 mV/s, 10mV/s, 20mV/s, 50mV/s, 100mV/s respectively, whereas the specific capacitance value for the MoS_2 electrode is 113 F/g at 5mV/s. Firmiano et al. reported specific capacitance value of medium concentration MoS_2 and rGO was 265 F/g at 10 mV/sec scan rate whereas specific capacitance value of our sample at the same scan rate is 376 F/g.[55] This might be due to high degree of exfoliation of materials in NMP which gives well dispersed ultrathin nanosheets of

MoS_2 and rGO. Figure10 (b) represent the CV graphs of MoS_2 and MoS_2/rGO hybrid electrode at 5 mV/s scan rate. Changes of areal capacitance value of the hybrid electrode material with scan rate are shown in the figure 10(c).A plot of C/C_0 vs cycle numbers is shown in the figure 10(d), which shows almost 95% retention in the areal capacitance value over 250 cycles. The hybrid material exhibits a high energy density of 5.71 mWh/cm^2 and a power density of 54.1 mW/cm^2.

4) Few layered vanadyl phosphate nano sheets-MWCNT hybrid as an electrode material for supercapacitor application

It has been already seen that 2-dimensional nano materials are the suitable choice for the supercapacitor application due to their large specific surface area, electrochemical active sites, micromechanical flexibility, expedite ion migration channel properties. Free standing hybrid films of functionalized MWCNT (–COOH group) and α-Vanadyl phosphates ($VOPO_4$. $2H_2O$) are prepared by vacuum filtering. Bulk vanadyl phosphate dihydrate ($VOPO_4$,$2H_2O$) was prepared refluxed at 110 ^{0}C for 16 h. Bulk vanadyl phosphate dihydrate was dispersed into 2-propanol with initial concentration 1mg/ml. Thereafter the dispersion was ultrasonicated by bath sonication for 15 minutes to get vanadyl phosphate nano sheets, the resulting well dispersed nano sheets was used to make composite films.

MWCNT-Vanadyl phosphate hybrid films were prepared by filtering an appropriate amount of mixed dispersion through polyvinylidene fluoride (PVDF) filtration membrane (Millipore, durapore membrane filters, and 100 nm pore size). The deposited hybrid films were dried overnight under vacuum at 50^0 C. Films were peeled off the filter membrane to get free standing hybrid films.

We have done powder X-ray diffraction (XRD) and Raman study to characterize as prepared $VOPO_4.2H_2O$ as shown in Fig.1(a), the X-ray diffraction pattern of as prepared vanadyl phosphate dehydrate shows a set of diffraction peaks at 2θ= 12.3^0, 24.9^{0}and 28.7^0 corresponding to (001),(002) and (102) planes with d values 0.71nm,0.36 nm,0.32 nm respectively. The formation of α phase of $VOPO_4.2H_2O$ have confirmed from the XRD (JCPDS card No.84-0111) pattern. The band at 950 cm^{-1} in the Raman spectrum (Figure 1b)for as prepared $VOPO_4.2H_2O$ is corresponds to symmetric stretching vibration ν_1 (PO_4) which shifted to lower wave number at 537 cm^{-1} for exfoliated $VOPO_4$. [56] This shift is due to breaking of hydrogen bonds from oxygen atoms of the P-O bond in $VOPO_4$.The bands due to symmetric bending vibrations $\nu 4$ (PO_4) at 550 and 580 cm^{-1} also present in Raman

spectrum for both as prepared and exfoliated vanadyl phosphate. The band at 1050 cm $^{-1}$ is corresponding to V=O stretching mode. The Raman spectra confirmed that there is no obvious change in in plane structure of $VOPO_4$.

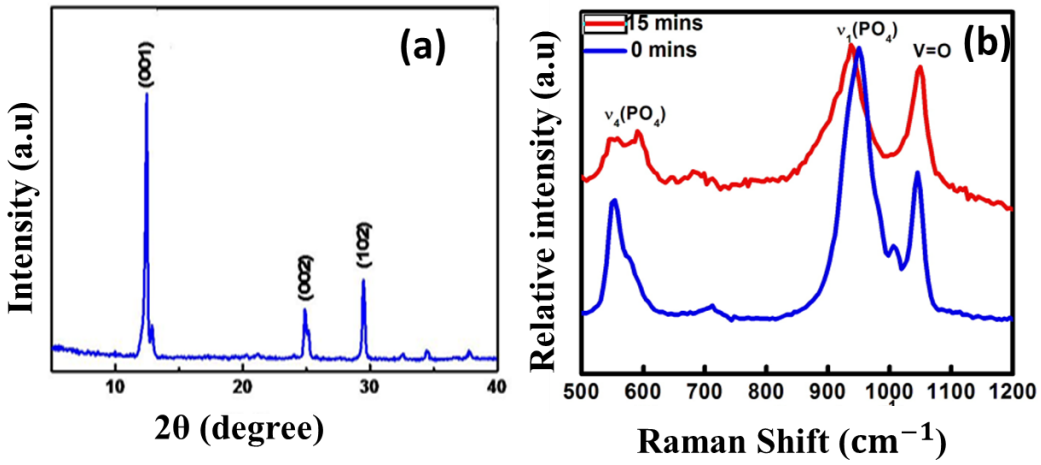

Figure11. (a) Powder XRD pattern of as prepared $VOPO_4.2H_2O$, and (b) Raman spectra of as prepared and exfoliated $VOPO_4.2H_2O$.

The SEM image shown in the figure 12(a) of exfoliated $VOPO_4$ which shows graphene like morphology of $VOPO_4$ after 15 mints sonication in 2 propanol. Figure 12(b) shows the surface and cross sectional part of a broken MWCNT film and 12(c) is the SEM image of MWCNT-$VOPO_4$ composite. This clearly shows the excellent mixing of $VOPO_4$ nano sheets into the MWCNT network and is uniformly distributed.

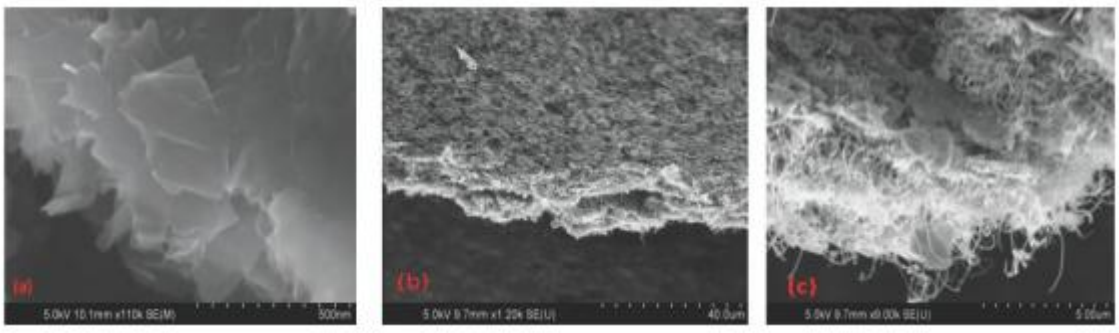

Figure12. FESEM images of exfoliated $VOPO_4$ (a), MWCNT film (b), MWCNT-$VOPO_4$ hybrid film (c).

To evaluate the performance of MWCNT-$VOPO_4$ hybrid films as electrode of supercapacitor, we have performed cyclic voltammetry (CV), galvanostatic charge-discharge (CD), and electrochemical impedance spectroscopy (EIS) tests using a two electrode system. Figure

13(a) shows the CV curves of hybrid electrodes at different scan rates 5mV/s to 100 mV/s with a voltage range -2.4 V to +2.4V. Redox peaks are observed in CV curve at about (+/-) 1V. The specific capacitance of hybrid electrodes was up to the 236 F/g at the scan rate 5 mV/s much higher than that of pure MWCNT electrodes (49 F/g) at the same scan rate. CV measurements of pure MWCNT electrode are also tested which reveals the performance of hybrid electrode over the pure MWCNT electrode (Fig.13b). The specific capacitance values calculated from the CV curves to be 236, 179, 87, and 59 F/g at 5, 10, 50, and 100 mV/sec scan rates respectively for hybrid materials. However the value of specific capacitance for pure MWCNT electrode at 5 mV/sec scan rate is 49 F/g. From the charging discharging curves (Fig 13c) and (Fig 13d) the value of specific capacitance of pure MWCNT electrodes and hybrid electrodes were found to be 3F/g and 82 F/g at current density 1 A/g respectively. The supercapacitor based on hybrid materials delivers a high energy density of 65.6 Wh/Kg at a power density 1476 W/Kg.

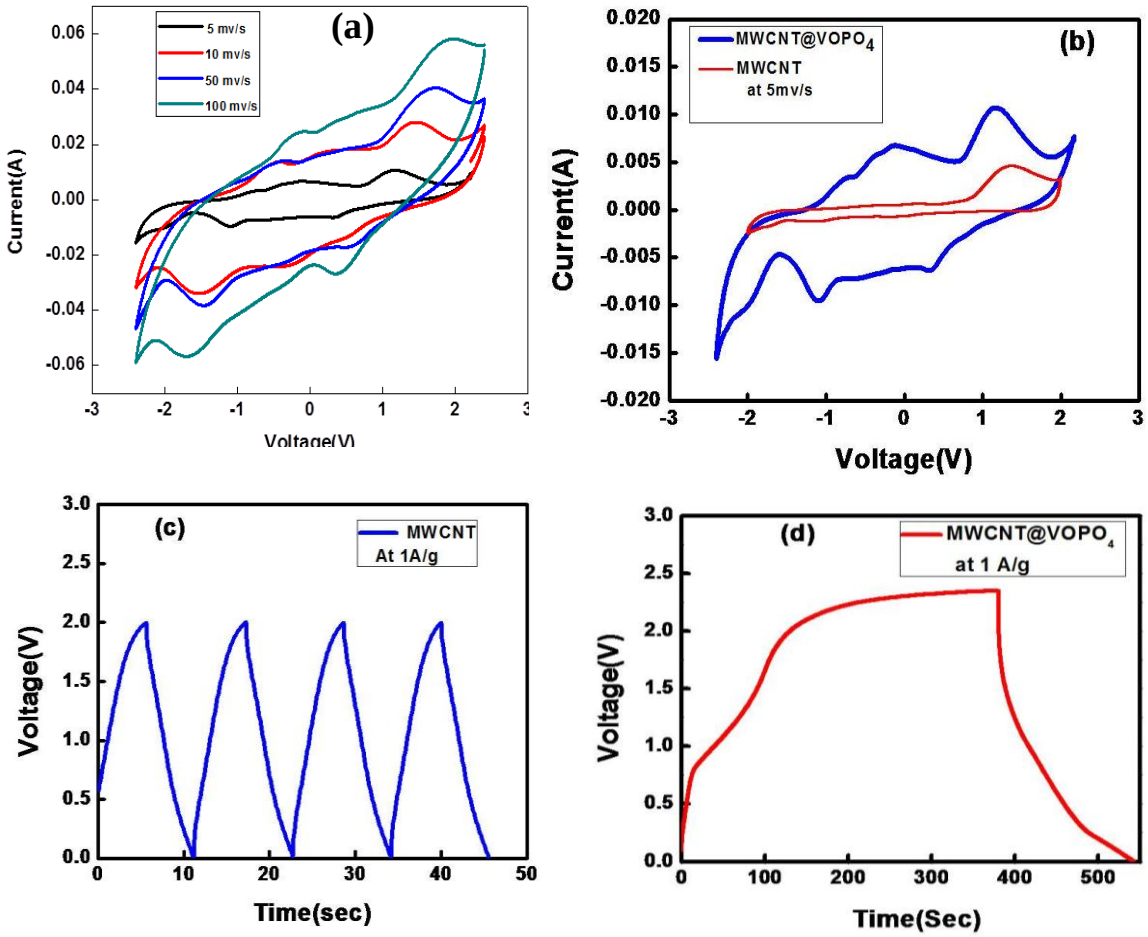

Figure13. CV curves of hybrid electrodes at different scan rates (a), CV curves of pure MWCNT and hybrid electrodes at 5 mV/s (b), charging discharging curves of pure MWCNT(c) and hybrid electrodes (d) at 1A/g.

5. Few-layered MnO_2/SWCNT hybrid in-plane supercapacitor with high energy density

In this present work we have synthesized few layered MnO_2 nanosheets by mixed solvent exfoliation process for the application as electrode material of in-plane supercapacitor. In planner supercapacitors, requirement of a separator is eliminated because the electrolyte ions are transported two-dimensionally. Yi Xie and his co-worker already reported few layered VS_2 based in-planer supercapacitors with high two dimensional conductivity obtained high areal capacitance of 4760 μF/cm^2. [17] Recently, Han Xiao et.al reported Phosphorene and Graphene Inter digital Micro-supercapacitors with capacitance of 9.8 mF/ cm^2. [57]

Here we present a mixed solvent exfoliation of α-MnO_2 nano sheets for high performance planer supercapacitors. The patterns of the hybrids were directly fabricated by (50: 50 wt %) mixture of MnO_2 and SWCNT dispersions with the help of a customized mask, and directly transferred onto a flexible PET substrate. In particular, the planar structures supercapacitors constructed by α-MnO_2 nanosheets integrated with SWCNT enhanced the electrochemical performances because of high electrochemically active surfaces for absorption/desorption of the electrolyte ions during charging–discharging process. In addition, the α-MnO_2 nanosheets also provide great active centres for the pseudocapacitive reactions contributions.

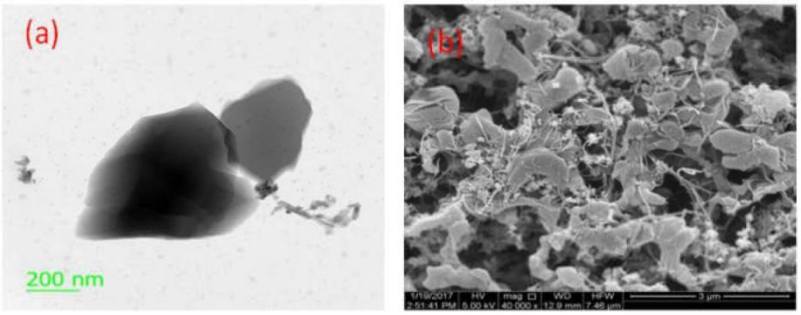

Figure 14. (a)TEM images of MnO_2, (b) FESEM images of MnO_2 /SWCNT hybrid

Low magnification TEM image (Fig 14.a) of the MnO_2 shows the formation of two dimensional nano sheets of lateral dimension of 300nm to 400 nm. The surface morphology of samples were characterized by FE-SEM. FESEM image of the thin films made by the composite materials displays in the fig.14(b) showed that the MnO_2 nano sheets were uniformly distributed in the CNT platforms. Fig.3 (a)-(f) shows the electrochemical performance of the as-fabricated in-plane supercapacitor based on MnO_2/SWCNT composite. Fig.15 (a)-(f) shows the electrochemical performance of the as-fabricated in-plane

supercapacitor based on MnO_2/SWCNT composite. The as-manufactured micro-supercapacitor based on few layered MnO_2 and SWCNT hybrid with PVA/H_2SO_4 solid state electrolyte have combine advantages of MnO_2 (pseudo nature) and SWCNT (EDLC nature) and as a result displayed excellent specific capacitance of 560.22 F/g with significant energy density of 77.80 Wh/kg and excellent cycling stability even after 1000 cycles. In addition, it showed outstanding flexibility with very stable performance under different bending conditions. Therefore, MnO_2/SWCNT hybrids in-plane micro capacitor is a good choice as next-generation flexible portable energy storage device applications.

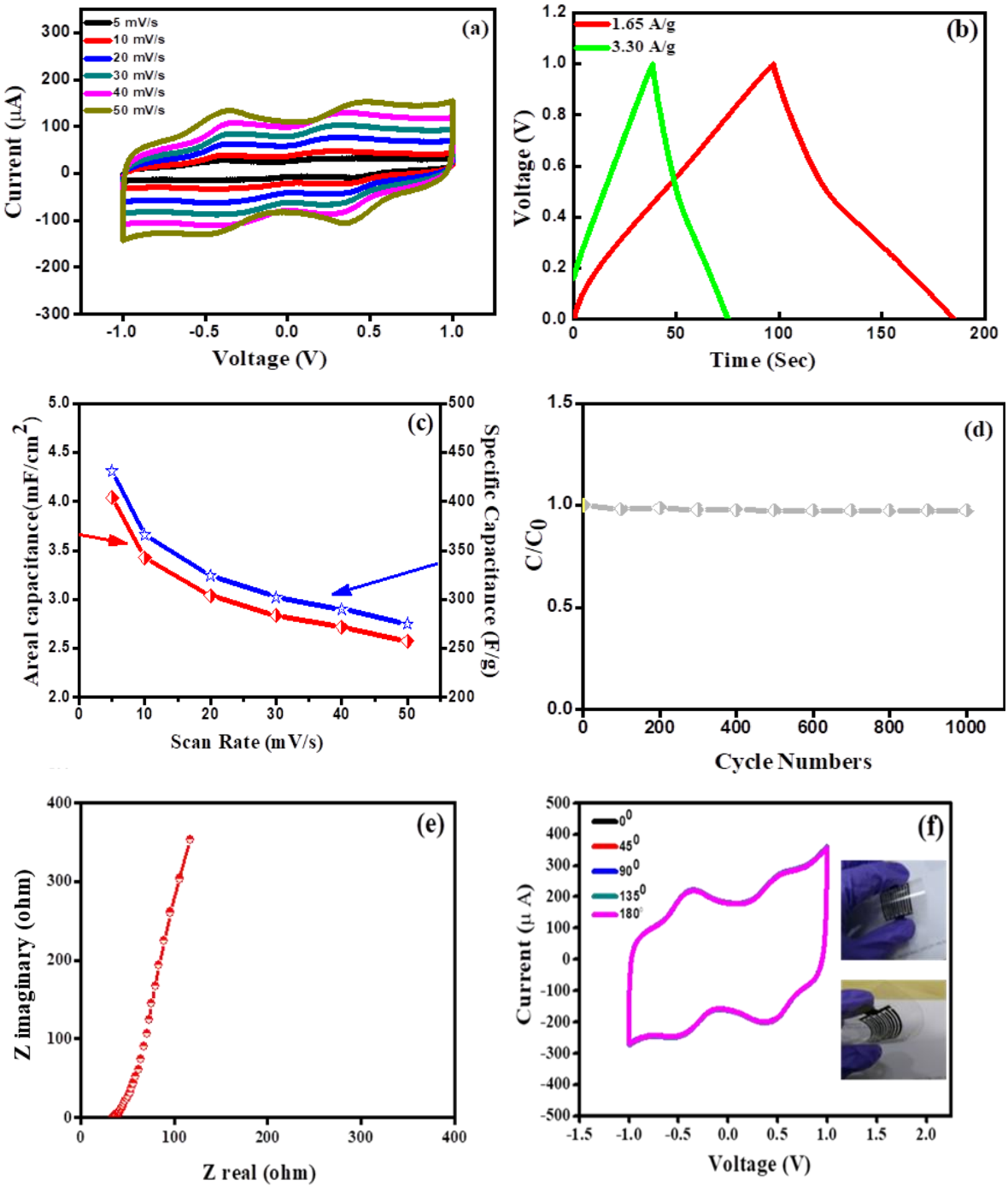

Figure 15. CV at different scan rates (a), Galvanostatic charge–discharge curves at different current density (b) specific capacitance and areal capacitance at different scan rates (c), Cycle stability graph (d), Nyquist plot (e), and CV curves tested at 100 mV s^{-1} under different bending angels (f).

5. Conclusions

The present thesis work obtained significant information about the large scale production of 2D materials via mixed solvent exfoliation as well as hydro (solvo) thermal process. The dispersion of 2D nanosheets allowed us to make thin films of nanosheets and their hybrids with carbonaceous nanostructure by vacuum filtration with thickness ranging from a few nanometers to micrometers. These films can be deposited on different substrates required for flexible supercapacitor electrode fabrication. Further, the variation of composition of the composite electrode materials helped to enhance the performance of the electrode materials. Our findings represent a promising direction and significant steps towards fabricate the flexible supercapacitors with high energy density using 2D nano sheets of various materials.

6. Acknowledgments

I sincerely acknowledge my supervisor Dr. Sukanta De from Presidency University, Kolkata for his kind guidance and useful discussions and valuable suggestions during my research work. I have been very fortunate to work under your guidance. I would like to express my profound thanks to Prof. Arabinda Nayak, and Dr. Rabindranath Gayen for their generous help in course work, research projects and support in experimental setup and laboratory issues.

I would like to express my deepest gratitude to my wife Dr. Shreyasi Pal for her unconditional support and constant encouragement in both of my Ph.D. study and being in my life. I am really grateful to her for keeping such patience to review all of my research documents line by line. Her constructive advices and scientific suggestions help me a lot. Finally, I would like to thank my parents and parents in laws for their love and support. Especially I also should express my deepest appreciations to my father in law for his supporting and motivated speech which cheer me always.

List of papers related to thesis:

1. Hydrothermally synthesized $BiVO_4$–reduced graphene oxide nanocomposite as a high performance supercapacitor electrode with excellent cycle stability, **Shibsankar Dutta**, Shreyasi Pal and Sukanta De, *New J. Chem.***,** 2018, 42**,** 10161-10166.
2. MoS_2 Nanosheet/rGO Hybrid: An Electrode Material for High Performance Thin Film Supercapacitor, **Shibsankar Dutta,** Sukanta De, *Mater. Today*, 2018 5 9771–5
3. Few layered vanadyl phosphate nano sheets-MWCNT hybrid as an electrode material for supercapacitor application, **Shibsankar Dutta,** Sukanta De, *AIP Conf. Proc.*, 2016, 1728, 020479.
4. Few-layered MnO_2/SWCNT hybrid in-plane supercapacitor with high energy density, **Shibsankar Dutta**, Shreyasi Pal and Sukanta De, *AIP Conf. Proc.* ,2018, 1953, 030145
5. Scalable Mixed Solvent Assisted Transition Metal Oxides Nanosheets Exfoliations and Their Composites with SWCNT towards the Fabrication of Flexible Supercapacitors Endowed with High Energy Density, **Shibsankar Dutta**, Shreyasi Pal and Sukanta De, *ACS Appl. Nano Mater*.(Communicated).

Papers not related to thesis:

1. Magnetic field induced electrochemical performance enhancement in reduced graphene oxide anchored Fe_3O_4 nanoparticle hybrid based supercapacitor, Shreyasi Pal,Sumit Majumder,**Shibsankar Dutta**,Sangam Banerjee,Biswarup Satpati, and Sukanta De, *J. Phys. D: Appl. Phys.*, 2018, 51 375501.
2. Development of an effective electrochemical platform for highly sensitive DNA detection using MoS_2 -polyaniline nanocomposites, **Shibsankar Dutta** , Ankan Dutta Chowdhury , Sangita Biswas , Enoch Y. Park , Nidhi Agnihotri , Amitabha De , Sukanta De, *Biochemical Engineering Journal*, 2018 ,140, 130–139.
3. Efficient Flexible White-Light Photodetectors Based On BiFeO3 Nanoparticles, Suchanda Mondal, Kajari Dutta, **Shibsankar Dutta**, Debnarayan Jana, Adam G. Kelly, and Sukanta De, *ACS Appl. Nano Mater.*, 2018, *1* (2), 625–631.
4. Highly efficient photocatalytic activity of CuO quantum dot decorated rGO nanocomposites, **Shibsankar Dutta**, Kajari Das, Kaushik Chakrabarti, D. Jana,S K De and Sukanta De, *J. Phys. D: Appl. Phys.*, 2016, 49, 315107.

5. Few layered MoO_3 nano sheets-SWCNT composite thin film as supercapacitor electrode, **Shibsankar Dutta**, Jasim Akther and Sukanta De, *AIP Conf. Proc.*, 2017, 1832, 050113.
6. One-dimensional α-MoO_3 nanorods for high energy density pseudocapacitor, **Shibsankar Dutta**, Shreyasi Pal and Sukanta De, *AIP Conf. Proc*, 2018,1942, 140086.
7. Synthesis of rGO@ZnS nanocomposites for visible light assisted high photocatalytic performance, Shibsankar Dutta, Subrata Mondal and Sukanta De, *Invertis Journal of Renewable Energy*, 2017, 7, 64-68.
8. A facile hydrothermal approach to synthesize rGO/$BiVO_4$ photocatalysts for visible light induced degradation of RhB dye, Shreyasi Pal, **Shibsankar Dutta** and Sukanta De, *AIP Conf. Proc*, 2018, 1953(1):030205.
9. Synthesis of MoS_2/rGO nanosheets hybrid materials for enhanced visible light assisted photocatalytic activity, Shreyasi Pal, **Shibsankar Dutta** and Sukanta De, *AIP Conf. Proc*, 2018, 1942(1):050129.

Conferences /Seminars/Workshops

1) ***"A one day seminar on "Basic physics to Contemporary Research"*** Organized by Department of Physics, Jadavpur University, 18th march 2015.
2) **"*Physics and Applied Mathematics Researchers' Meet-2015"*,** Organized by Physics and Applied mathematics unit, Indian Statistical Institute, Kolkata, India, 18th -20th march 2015.
3) ***"Workshop On Indian Innovations In Materials Research: New Materials And Processes (IIMR-15)*** , Organized jointly by CSIR-CGCRI & IAPQR, KOLKATA, 25th -27th June, 2015.
4) ***"International conference on Recent Advances in Nano Science and Technology (RAINSAT- 2015)",*** July 8th – 10th, 2015, in association with CSIR-Central Leather Research Institute, India, organized by Sathyabama University.
5) **"*Condensed Matter Days 2015 (CMDAYS 2015)*"**,Organised by Department of physics,Visva-Bharati, Santiniketan ,West Bengal, August 27th -29th, 2015
6) ***"International conference on Condensed Matter & Applied Physics (ICC-2015)",*** organized by Govt. Engineering college Bikaner & Ceramic Electrical Research & Development Centre,Bikaner, Rajasthan, October 30th- 31th ,2015

7) ***"International conference on Nanomaterias and nanotechnology,(NANO-15),***organized by Rangasamy College of Technology, Tiruchengode, India, December 7^{th}-10^{th} 2015.

8) ***"International conference on Nanoscience, Nanotechnology & Advanced Materials(NANOS 2015)",*** organized by Department of Chemistry, Gitam Institute of Science,GitamUniversity ,Rushikonda,Visakhapatnam,Andhra Pradesh, December 14^{th}-17^{th} ,2015.

9) **"*Functional Materials: Recent Trends, One day symposium"*** , organized by department of Physics Presidency University,29^{th} January, 2016.

10) ***"23rd West Bengal State Science & Technology congress 2016",*** organized by Presidency University, 28^{th} -29^{th} February, 2016.

11) ***"National Conference on Modern Trends in condensed Matter Physics (MTCMP-2016)",*** Organized by department of Physics, West Bengal State University Barasat,Kolkata, 11^{th} -12^{th} march, 2016.

12) **"*National Conference on Emerging Trends in condensed Matter Physics & material science (ETCMPMS-2016*),** Organized by department of Physics, University of Kalyani,18^{th} -19^{th} March, 2016.

13) **One day Seminar on *"Some Recent Trends in Research in Physics(SRTRP-2016)"*** ,Organized by department of Physics,Jadavpur University, Kolkata, 21^{st} March, 2016.

14) **"*UGC sponsored National level Seminar*",** Organized by Department of Industrial Chemistry, Ramkrishna Mission Vidyamandira in collaboration with School of Material Science & Nanotechnology, Jadavpur University,28^{th} -29^{th} march 2016.

15) ***"National Conference on Nanotechnology: Materials and Applications (NCoN:M&A)",*** Organized by School of materials science and Nanotechnology,Jadavpur University,16^{th}-17^{th} June 2016.

16) **"** ***International Conference on Functional Nanomaterials (IC-FNM 2016)"*** **,** Organized by CoE on Micro-structurally Designed Advanced Materials under TEQIP (II) and (MND SMSE) of Indian Institute of Engineering Science and Technology(IIEST),Shibpur,India, 28^{th} -29^{th} September 2016.

17) ***"61st DAE solid state physics symposium 2016",*** Organized by KIIT university, Bhubaneswar, 26^{th}- 30^{th} December, 2016.

18) ***"Fourth International Symposium on Semiconductor Materials and Devices (ISSMD 4)",*** Organized by School of materials science and Nanotechnology, Jadavpur University, 8^{th}-10^{th} June 2017.

19) ***"National Conference on Recent Trends in Condensed Matter Physics"*** , Organized by Bose Institute, Kolkata 31st October – 3rd November 2017.

20) ***"International conference on Condensed Matter Physics",*** Organized by Physics and Applied mathematics unit, Indian Statistical Institute, Kolkata, India, November 14 -16, 2017.

21) ***"International conference on Condensed Matter & Applied Physics (ICC-2017)",*** organized by Govt. Engineering college Bikaner & Ceramic Electrical Research & Development Centre, Bikaner, Rajasthan, 24th -25th November 2017.

22) ***"Science Academies Lecture Workshop on Modern Trends in Chemistry and Physics"*** , Organized by Department of Physics Bhairab Ganguly College, 17th -19th December.

23) ***"62nd DAE solid state physics symposium 2017",*** Organized by Bhaba Atomic Research Centre, Mumbai, 26th- 30th December, 2017.

References

1. H. Wang, H. S. Casalongue, Y. Liang and H. Dai, *J. Am.Chem. Soc.*2010, **132**, 7472–7477.
2. M. Winter and R. J. Brodd, *Chem. Rev.*2004, **104**, 4245– 4270.
3. J. Huang, B. G. Sumpter and V. Meunier, Angew. Chem., Int. Ed., 2008, **47**, 520–524
4. J. Gamby, P. Taberna, P. Simon, J. Fauvarque and M. Chesneau, *J. Power Sources* 2001, **101**, 109–116.
5. D. N. Futaba, K. Hata, T. Yamada, T. Hiraoka, Y. Hayamizu,Y. Kakudate, O. Tanaike, H. Hatori, M. Yumura and S. Iijima, *Nat. Mater.* 2006, **5**, 987–994.
6. Y. Wang, Z. Shi, Y. Huang, Y. Ma, C. Wang, M. Chen and Y. Chen, *J. Phys. Chem. C* 2009, **113**, 13103–13107.
7. L. L. Zhang, R. Zhou and X. Zhao, *J. Mater. Chem.* 2010, **20**, 5983–5992.
8. W. Tang, L. Liu, S. Tian, L. Li, Y. Yue, Y. Wu and K. Zhu, *Chem. Commun*. 2011 **47**, 10058-10060.
9. F. Luan, G. Wang, Y. Ling, X. Lu, H. Wang, Y. Tong, X.X. Liu and Y. Li, *Nanoscale* 2013, **5**, 7984-7990.
10. C.C. Hu, K.H. Chang, M.C. Lin and Y.T. Wu, *Nano Lett.* 2006, **6**, 2690-2695.
11. X. Lu, G. Wang, T. Zhai, M. Yu, J. Gan, Y. Tong and Y. Li, *Nano Lett.* 2012, **12**, 1690-1696.

12. X. Lu, T. Zhai, X. Zhang, Y. Shen, L. Yuan, B. Hu, L. Gong, J. Chen, Y. Gao, J. Zhou, Y. Tong and Z. L. Wang, *Adv. Mater.* 2012, **24**, 938-944.
13. G. Yu, L. Hu, N. Liu, H. Wang, M. Vosgueritchian, Y. Yang, Y. Cui and Z. Bao, *Nano Lett.*2011, **11**, 4438-4442.
14. G. Yu, L. Hu, M. Vosgueritchian, H. Wang, X. Xie, J. R. McDonough, X. Cui, Y. Cui and Z. Bao, *Nano Lett.* 2011, **11**, 2905-2911.
15. L. Wu, R. Li, J. Guo, C. Zhou, W. Zhang, C. Wang, Y. Huang, Y. Li and J. Liu, *AIP Adv.*2013, **3**, 082129.
16. L. Peng, X. Peng, B. Liu, C. Wu, Y. Xie and G. Yu, *Nano Lett.*2013, **13**, 2151-2157.
17. J. Feng, X. Sun, C. Wu, L. Peng, C. Lin, S. Hu, J. Yang and Y. Xie, *J. Am. Chem. Soc.* 2011, **133**, 17832-17838.
18. J. Xie, X. Sun, N. Zhang, K. Xu, M. Zhou and Y. Xie, *Nano Energy* 2013**, 2**, 65-74.
19. J. Yan, Z. Fan, W. Sun, G. Ning, T. Wei, Q. Zhang, R. Zhang, L. Zhi and F. Wei, *Adv. Funct. Mater.*2012, **22**, 2632-2641.
20. V. Gupta, T. Kusahara, H. Toyama, S. Gupta and N. Miura, *Electrochem. Commun.* 2012, **9**, 2315-2319.
21. H. Wang, Q. Hao, X. Yang, L. Lu and X. Wang, *Nanoscale* 2010, **2**, 2164-2170.
22. K. Jurewicz, S. Delpeux, V. Bertagna, F. Beguin and E. Frackowiak, *Chem. Phys. Lett.* 2001, **347**, 36-40.
23. J. Tao, N. Liu, W. Ma, L. Ding, L. Li, J. Su and Y. Gao, *Sci. Rep.* 2013, **3**, 2286.
24. A. Laforgue, P. Simon, C. Sarrazin, J. F. Fauvarque, *J. Power Sources* 1999, **80**, 142-148.
25. J. J. Yoo, K. Balakrishnan, J. Huang, V. Meunier, B. G. Sumpter, A. Srivastava, M. Conway, A. L. M. Reddy, J. Yu, R. Vajtai and P. M. Ajayan, *Nano Lett.* 2011, **11**, 1423-1427.
26. X. Huang, X. Qi, F. Boey and H. Zhang, *Chem. Soc. Rev.* 2012, **41**, 666-686.
27. A. K. Geim and K. S. Novoselov, *Nat. Mater.* 2007, **6**, 183-191.
28. X. Huang, C.Tan, Z. Yin, and H. Zhang, *Adv. Mater.* 2014, **26**, 2185-2204.
29. F. Bonaccorso, L. Colombo, G. Yu, M. Stoller, V. Tozzini, A. C. Ferrari, R. S. Ruoff, V. Pellegrini. *Science* 2015, **41**, 347.
30. S. Dutta, S. Pal, and S. De, *New J. Chem.* 2018, **42**, 10161-10166.
31. G. Wang, X.G. Zhu, Y.Y. Sun, Y.Y. Li, T. Zhang, J. Wen, X.Chen, K. He, L.L. Wang, X.C. Ma, J.F. Jia, S. B. Zhang and Q.K. Xue,. *Adv. Mater.* 2011, **23**, 2929-2932.

32. C. Y. Zhi, Y. Bando, C. C. Tang, H. Kuwahara, D. Golberg, *Adv. Mater.* 2009, **21**, 2889-2893.
33. B. Radisavljevic, A. Radenovic, J. Brivio, V. Giacometti, A. Kis, *Nat. Nanotechnol.* 2011, **6**, 147-150.
34. W. J. Yu, S. Y. Lee, S. H. Chae, D. Perello, G. H. Han, M. Yun and Y. H. Lee, *Nano Lett.* 2011, **11**, 1344-1350.
35. S. Yin, Y. Zhang, J. Kong, C. Zou, C. M. Li, X. Lu, J. Ma, F. Y. C. Boey, X. Chen, *ACS Nano.* 2011, **5**, 3831-3838.
36. K.Chang, and W.Chen,.*ACS Nano*. 2011, **5**, 4720-4728.
37. S.-L. Chou, J.Z. Wang, S.-Y. Chew, H.-K. Liu and S.-X. Dou, *Electrochem. Commun.* 2008, **10**, 1724–1727.
38. M. Jin, G. Han, Y. Chang, H. Zhao and H. Zhang, *Electrochim. Acta*. 2011, **56**, 9838–9845.
39. M. C. K. Sellers, N. P. Zussblatt and C. P. Marsh, *Electrochem. Commun.* 2012, **18**, 58–61.
40. K. S. Novoselov, A. K. Geim, S. V. Morozov, D. Jiang, Y. Zhang, S. V. Dubonos, I. V. Grigorieva and A. A. Firsov, *Science* 2004, **306**, 666–669.
41. M. D. Stoller, S. Park, Y. Zhu, J. and R. S. Ruoff, *Nano Lett.* 2008, **8**, 3498–3502.
42. L. Zhang and G. Shi, *J. Phys. Chem. C*, 2011, **115**, 17206–17212.
43. K Zhou , W Zhou, X Liu , Y Sang , S Ji , W Li , J Lu , L Li , W Niu , H Liu and S Chen, *Nano Energy* 2015 **12**, 510–520.
44. X. Dong, L. Wang, D. Wang, C. Li and J. Jin, *Langmuir* 2012, **28**, 293–298.
45. C. Wu, X. Lu, L. Peng, K. Xu, X. Peng, J. Huang, G. Yu and Y. Xie, *Nat. Commun*., 2013, **4**, 2431.
46. H. Wang, H. Yi, X Chen and X. Wang, *J. Mater. Chem. A* 2014, **2**, 3223-3230.
47. S. Ratha and C. S. Rout. *RSC Adv.* 2015, **5**, 86551-86557.
48. P. Taberna, P. Simon and J.F. Fauvarque, *Journal of the Electrochemical Society* 2003, **150**, A292-A300.
49. C. M. Hansen, *CRC, Boca Raton*, 2007**.**
50. J. N. Coleman, *Adv. Funct. Mater.* 2009, **19**, 3680-3695.
51. D. Hanlon, C. Backes, T. M. Higgins, M. Hughes, A. O'Neill, P. King, N. McEvoy, G. S. Duesberg, B. M. Sanchez, H. Pettersson, V. Nicolosi and J. N. Coleman, *Chem. Mater.* 2014, **26**, 1751–1763.

52. K. Kalantar-zadeh, J. Tang, M. Wang, K. L. Wang, A. Shailos, K. Galatsis, R. Kojima, V. Strong, A. Lech, W. Wlodarski and R. B. Kaner, *Nanoscale*, 2010, **2**, 429-433.
53. M. Osada, T. Sasaki, *J. Mater. Chem.*, 2009, **19**, 2503-2511.
54. S.J. Choi, J.S. Jang, H. J.Park, and I.D. Kim, *Adv. Funct. Mater.* 2017, 1606026.
55. E. G. Da Silveira Firmiano, et al. *Adv. Energy Mater* 2014, **4**, 1301380.
56. L. Benes, K. Melanova, M. Trchova, P. Capkova, and P. Matejka, *Eur. J. Inorg. Chem*. 1999, **1999**, 2289-2294.
57. H. Xiao et al. *ACS Nano.* 2017, **11**, 7284-7292.